

## Spontaneous emission control of single quantum dots in bottom-up nanowire waveguides

Gabriele Bulgarini,<sup>1,a),b)</sup> Michael E. Reimer,<sup>1,a)</sup> Tilman Zehender,<sup>2</sup> Moira Hocevar,<sup>1</sup> Erik P. A. M. Bakkers,<sup>1,2</sup> Leo P. Kouwenhoven,<sup>1</sup> and Valery Zwiller<sup>1</sup>

<sup>1</sup>Kavli Institute of Nanoscience, Delft University of Technology, Delft, The Netherlands

<sup>2</sup>Eindhoven University of Technology, Eindhoven, The Netherlands

(Received 24 January 2012; accepted 28 February 2012; published online 20 March 2012)

Nanowire waveguides with controlled shape are promising for engineering the collection efficiency of quantum light sources. We investigate the exciton lifetime in individual InAsP quantum dots, perfectly positioned on-axis of InP nanowire waveguides. We demonstrate control over the quantum dot spontaneous emission by varying the nanowire diameter in e-beam patterned arrays, which modifies the coupling efficiency of the emitter to the fundamental waveguide mode. The spontaneous emission rate is inhibited by a factor of 12 in thin nanowires compared to nanowires with optimized waveguide diameter. From the measured inhibition factor, we determine a high radiative yield exceeding 92% in bottom-up grown nanowires. © 2012 American Institute of Physics. [<http://dx.doi.org/10.1063/1.3694935>]

Nanowire waveguides enable the efficient collection of single photons emitted from solid-state sources with the promise to reach efficiencies larger than 90%. High collection efficiency has been demonstrated for self-assembled quantum dots in top-down etched nanowires,<sup>1</sup> single quantum dots in bottom-up grown nanowires,<sup>2</sup> and color-centers in etched diamond nanowires.<sup>3</sup> One of the key parameters in designing a waveguide structure is the ratio between the nanowire diameter,  $D$ , and the emission wavelength,  $\lambda$ . Under optimum waveguide conditions ( $D/\lambda = 0.22$  for GaAs (Ref. 4) and 0.23 for InP (Ref. 2) nanowires), emitted photons are funneled into the fundamental waveguide mode confined in the nanowire. As a result, the emission is very directional and can be efficiently collected with limited numerical aperture objectives.<sup>4</sup> In contrast, at low  $D/\lambda$  ratios, optical modes are no longer confined in the nanowire and the source only couples to a continuum of non-guided radiative modes yielding a non-directional emission pattern and inefficient collection of the light.

Bleuse *et al.*<sup>5</sup> demonstrated that the spontaneous emission rate  $\Gamma$ , defined as the inverse of the emission lifetime  $\tau$ , depends strongly on the nanowire diameter. The spontaneous emission rate for diameters optimized for the waveguide approaches emission rates for the same emitter in a bulk matrix ( $\Gamma = 0.9 \times \Gamma_{\text{bulk}}$  for GaAs (Ref. 5)). Conversely, the spontaneous emission is suppressed at smaller nanowire diameters where the emitter weakly couples to waveguide modes in the nanowire. The spontaneous emission rate is further suppressed for randomly positioned quantum dots displaced with respect to the waveguide axis, which is thus far a common issue for self-assembled quantum dots in etched waveguides.<sup>1,5</sup> Here, we overcome this positioning issue by core-shell bottom-up growth of nanowire waveguides with quantum dots perfectly positioned on the waveguide axis. Our growth method enables independent control of the quan-

um dot location in the nanowire core and the total waveguide diameter set by the shell thickness. In this letter, we study the exciton lifetime for 50 individual quantum dots with  $D/\lambda$  ranging from 0.14 to 0.30. Importantly, we are able to accurately tune the waveguide diameter by controlling the nanowire interdistance in arrays patterned on a single chip, while maintaining the same dimensions of the nanowire core where the quantum dot is positioned.

InAsP quantum dots in InP nanowires are grown in a metal-organic vapor phase epitaxy reactor using the vapor-liquid-solid growth mechanism initiated with a gold catalyst. Electron-beam lithography is utilized for defining the gold catalyst size (25 and 50 nm in diameter) and positioning them in arrays<sup>6,7</sup> with a nanowire interdistance ranging from 0.8 to 5  $\mu\text{m}$ . Prior to growth, a two-step cleaning process including a *Piranha* etch and an in-situ anneal at 550 °C is performed in order to remove resist residues from the substrate.<sup>8</sup> The growth is initiated with the core of the InP nanowire at 420 °C, where an individual quantum dot is grown at half the nanowire length by adding arsenic to the system. The height of the quantum dot is defined by the growth time and is approximately 10 nm,<sup>9</sup> whereas the quantum dot diameter is determined by the size of the gold catalyst. Subsequently to the quantum dot growth, we increase the temperature to 500 °C in order to enhance radial growth compared to axial growth and surround the nanowire core with a homogenous InP shell. By varying the pitch of the nanowire array for a given catalyst size, we tune the shell growth rate. The shell thickness determines the final diameter of the nanowire waveguide.

Fig. 1(a) shows scanning electron micrographs of nanowires grown from 25 nm gold catalysts in arrays of different pitches. We observe that, as the nanowire length remains constant ( $\sim 7 \mu\text{m}$ ), the nanowire diameter enlarges by increasing the wire-to-wire distance ( $L$ ). At small  $L$ , nanowires grow in the competitive growth regime and compete in the collection of indium atoms diffusing on the substrate surface.<sup>10</sup> By increasing  $L$ , the collection area for each nanowire

<sup>a)</sup>These authors contributed equally to this work.

<sup>b)</sup>Electronic mail: g.bulgarini@tudelft.nl.

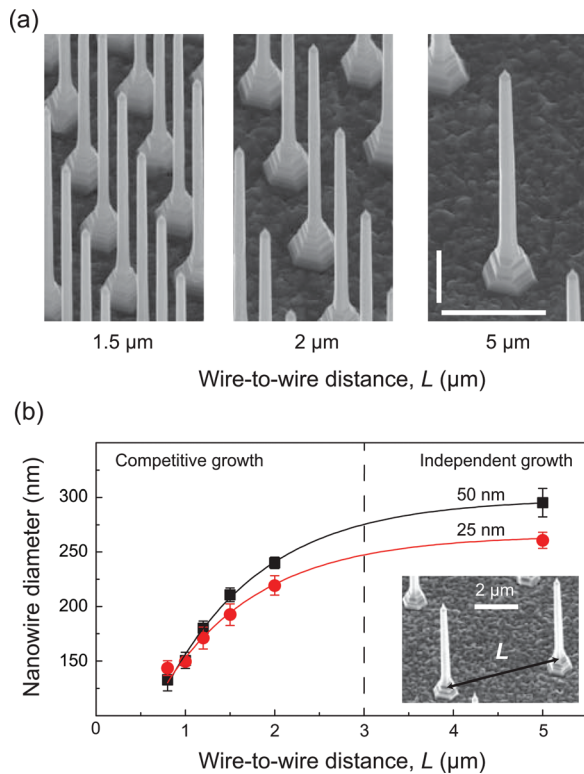


FIG. 1. (Color) (a) Scanning electron micrographs of nanowires grown on the same chip using 25 nm gold catalysts and varying pitch. All images were acquired at the same magnification with the sample tilted by  $30^\circ$  with respect to the electron beam. Vertical and horizontal scale bars represent  $2 \mu\text{m}$ . (b) Dependence of the nanowire diameter on the wire-to-wire distance for 25 nm (red circles) and 50 nm (black squares) gold catalysts. Inset shows the pitch of the growth array,  $L$ . We observe an increase of the nanowire diameter as  $L$  is enlarged from 0.8 to  $2 \mu\text{m}$  with a saturation at larger nanowire spacing. The dashed line indicates the transition from competitive to independent growth at  $L \sim 3 \mu\text{m}$ .

enlarges, resulting in an enhancement of the volume collected per nanowire owed by mass conservation as it has been previously reported for InAs (Ref. 10) and GaP (Ref. 11) nanowires. Finally, when the distance between nanowires exceeds the diffusion length of indium atoms, the growth rate becomes independent on the nanowire spacing and saturates. In our work, we exploit these two growth regimes to accurately control the nanowire waveguide diameter. In Fig. 1(b), we measure the average nanowire diameter at the quantum dot position for each growth array. We observe the transition from the competitive to independent growth regime at  $L \sim 3 \mu\text{m}$ .

Photoluminescence (PL) spectroscopy is utilized to study the spontaneous emission properties of single InAsP quantum dots in InP nanowire waveguides. Fig. 2(a) shows typical PL spectra of a single quantum dot as a function of the excitation power at 10 K, using a continuous-wave Ti:Sapphire laser at  $\lambda = 750 \text{ nm}$  and spot size of  $\sim 1 \mu\text{m}$ . We observe two emission peaks due to the exciton (X) recombination at 979.1 nm and the biexciton (XX) recombination at 979.6 nm, respectively. Fig. 2(b) shows the integrated emission intensity measured on a silicon CCD for the X and XX peak, respectively, as a function of the excitation power. Experimental data are fit with Poisson statistics using a linear and quadratic coefficient for X and XX, respectively, in order to accurately label the peaks. A PL spectrum at low excitation power is shown in Fig. 2(c).

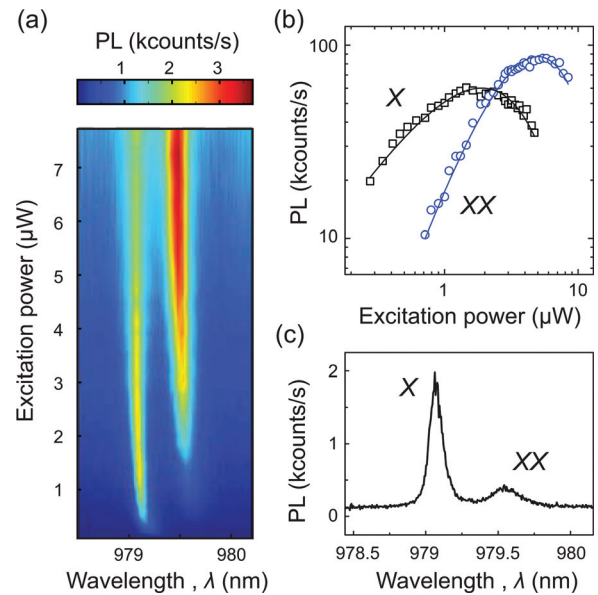


FIG. 2. (Color) (a) Power dependent PL spectroscopy of a single InAsP quantum dot in an InP nanowire. The intensity of PL emission is displayed as color. (b) Integrated PL intensity for exciton (X, black squares) and biexciton (XX, blue circles) emission peaks, fitted with Poisson statistics using linear and quadratic coefficients, respectively. (c) PL spectrum at low excitation power ( $0.8 \mu\text{W}$ ). The exciton emission exhibits a linewidth (FWHM) of  $120 \mu\text{eV}$ .

The exciton emission linewidth is  $120 \mu\text{eV}$  and is separated from the biexciton emission by  $0.65 \text{ meV}$ . The spectrum is representative of the quantum dots investigated in this work that exhibit a rather narrow distribution of exciton emission wavelength:  $975 \pm 5 \text{ nm}$ .

In the following, we filter the exciton peak in order to measure the exciton lifetime through time-resolved photoluminescence. Fig. 3 shows five photoluminescence decays measured on single quantum dots positioned in nanowires with different diameters, corresponding to different  $D/\lambda$  ratios. The quantum dot is now excited with 3 ps laser pulses using a repetition rate of 76 MHz and time-resolved PL is measured with a silicon avalanche photodiode. The background associated with the dark counts of the detector is subtracted from the measurements. The PL intensity (circles) is normalized to 1 for each measurement and the PL decays are fitted with mono-exponential decays displayed by blue lines. The exciton lifetime is significantly shortened by increasing  $D/\lambda$  from 0.14 to 0.24, since at larger diameters the quantum dot couples with higher efficiency to the fundamental waveguide mode of the nanowire. In contrast, at smaller nanowire diameters, the density of radiative modes available for the quantum dot is strongly reduced.

In Fig. 4, we plot the exciton lifetime for all investigated quantum dots with  $D/\lambda$  ratios ranging from 0.14 to 0.30. Each experimental data point refers to the exciton lifetime of a single quantum dot and the corresponding  $D/\lambda$  ratio is calculated from the exciton emission wavelength. At small  $D/\lambda$  (0.14–0.15), the quantum dot only couples to a continuum of non-guided radiative modes propagating away from the nanowire axis with a long recombination lifetime ( $\tau > 15 \text{ ns}$ ). By increasing  $D/\lambda$ , the quantum dot emits photons into the fundamental mode of the nanowire waveguide with an increased rate in comparison to non-guided modes.<sup>4</sup> Thus,

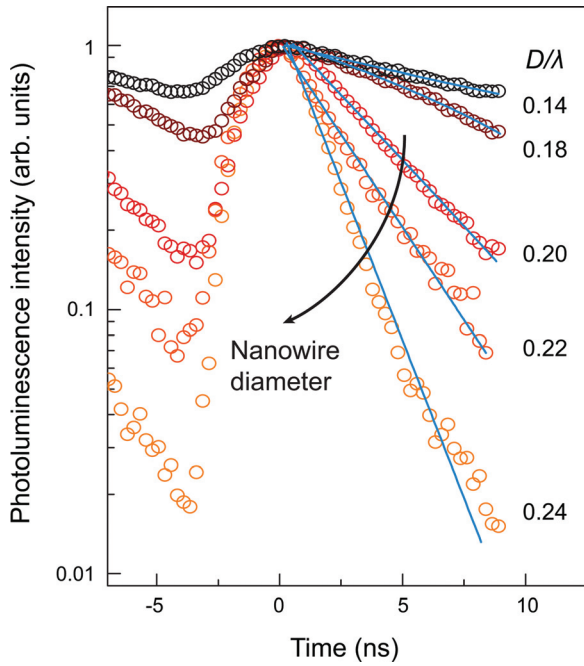


FIG. 3. (Color) Exciton lifetime measured via time-resolved photoluminescence on five different quantum dots embedded in nanowires with different diameters. The photoluminescence intensity (circles) is shown in a logarithmic scale and each curve is fitted with a mono-exponential decay (blue lines). As the nanowire diameter is increased, and accordingly the  $D/\lambda$  ratio, the quantum dot emission mode is confined in the nanowire and couples to the fundamental waveguide mode with an increased rate. The result is a significant shortening of the exciton lifetime.

the coupling of the quantum dot to this waveguide mode results in a remarkable shortening of the exciton lifetime until saturation occurs for  $D/\lambda$  ranging between 0.24 and 0.30. At saturation, the exciton lifetime approaches 1.7 ns as predicted for InAs quantum dots buried in a bulk InP matrix<sup>12</sup> (displayed by the red dashed dotted line). The observed behavior is consistent with calculations that assume an in-plane radiative dipole for the quantum dot,<sup>4</sup> which are experimentally confirmed in Ref. 5. Hence, we conclude that the dipole associated with the exciton transition is oriented perpendicular to the waveguide axis for quantum dots in bottom-up grown nanowires studied in this work. From the dipole orientation, combined with the quantum dot position on the nanowire axis,<sup>2</sup> a coupling efficiency to the fundamental waveguide mode above 95% is expected from fully vectorial calculations under optimum photonic confinement.<sup>5</sup> By comparing the exciton lifetime measured for  $D/\lambda \sim 0.245$  (dotted circle,  $\tau = 2.0 \pm 0.2$  ns) with that measured for  $D/\lambda \sim 0.14$  (black circle,  $\tau = 24.0 \pm 0.4$  ns), we obtain an inhibition factor of 12 for thinner nanowires. This inhibition of the spontaneous emission rate is solely due to suppression of the coupling to the fundamental waveguide mode.<sup>4</sup> Similar results have been demonstrated by using the bandgap of 2D photonic crystals,<sup>13,14</sup> 3D photonic crystals,<sup>15,16</sup> or with photonic nanowires.<sup>5</sup> In stark contrast to top-down etched photonic nanowires, the quantum dot emission in bottom-up grown nanowires is still clearly visible for diameters as small as 50-60 nm.<sup>9</sup> In the case of photonic nanowires with  $D < 120$  nm,<sup>5</sup> the quantum dot emission is totally suppressed, most likely due to surface non-radiative recombination enhanced by etching-related defects.

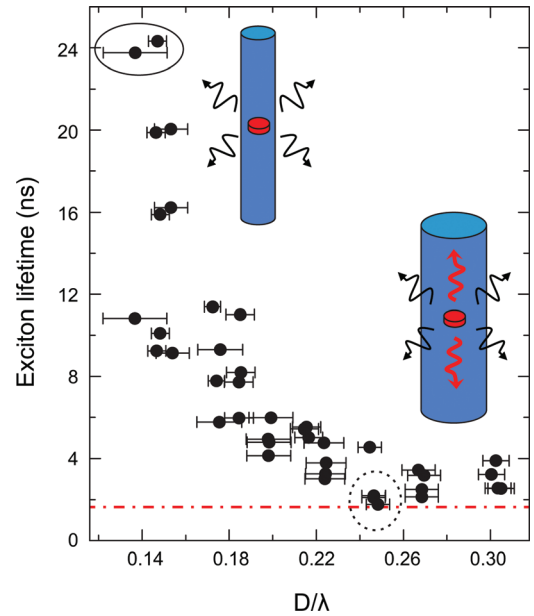


FIG. 4. (Color) Exciton lifetime for  $D/\lambda$  ratios ranging from 0.14 to 0.30. Each experimental point represents the exciton lifetime measured for a single quantum dot. The exciton lifetime is long for small nanowire diameters (black circle) and decreases as the fundamental waveguide mode becomes available for the emitter at larger diameters. We observe optimum photonic confinement conditions at  $D/\lambda \sim 0.245$ , where quantum dots exhibit a lifetime of 2 ns (dotted circle) which approaches the lifetime predicted for the same material system in bulk (red dashed dotted line). The suppression of the quantum dot coupling to waveguide modes that we observe for thin nanowires compared to nanowires having optimum waveguide conditions results in an inhibition factor of 12 for the spontaneous emission rate. Error bars are provided for  $D/\lambda$  ratio due to the variation of nanowire diameter measured within the same growth pattern.

We now estimate the radiative quantum efficiency of InAsP quantum dots in bottom-up grown nanowires. The long exciton lifetime that we measure in thin nanowires (i.e.,  $\tau = 24$  ns for  $D/\lambda \sim 0.14$ ) is suggestive of the high optical quality for quantum dots investigated in this work since non-radiative recombination processes act on time scales longer than 24 ns ( $\Gamma = 1/\tau = 42 \mu\text{s}^{-1}$ ). Since the total recombination rate,  $\Gamma$ , is composed of both radiative,  $\Gamma_R$ , and non-radiative,  $\Gamma_{NR}$ , decay channels,

$$\Gamma = \Gamma_R + \Gamma_{NR}, \quad (1)$$

the slow recombination rate that we measure for thin nanowires sets the highest limit of  $\Gamma_{NR} = 42 \mu\text{s}^{-1}$ . In reality, however,  $\Gamma_{NR}$  is lower since part of the measured recombination rate is originating from light emission. In order to calculate the radiative quantum efficiency,  $\eta = \Gamma_R/\Gamma$ , we analyze the recombination rate when the quantum dot couples to the fundamental waveguide mode of the nanowire and we assume that the non-radiative recombination rate,  $\Gamma_{NR}$ , is constant as a function of nanowire diameter. At  $D/\lambda \sim 0.245$ , the average measured lifetime is  $\tau = 2$  ns, corresponding to a recombination rate of  $\Gamma = 500 \mu\text{s}^{-1}$ . Thus, using  $\Gamma_{NR} = 42 \mu\text{s}^{-1}$  we infer from Eq. (1) that  $\Gamma_R = 458 \mu\text{s}^{-1}$ . As a result, we obtain a high radiative quantum efficiency,  $\eta = 92\%$ , which is the first experimental measurement for the efficiency of InAsP quantum dots in bottom-up grown nanowires and should be considered as a lower bound of the actual radiative quantum efficiency.

In this work, we have investigated the exciton spontaneous emission lifetime for single InAsP quantum dots positioned on the axis of InP nanowire waveguides. The bottom-up approach employed for the growth of nanowires enables us to analyze a wide range of diameters on the same chip. The e-beam positioning of gold catalysts allows for an accurate control of nanowire diameter during growth and for obtaining high uniformity within the same growth array. We have demonstrated that the spontaneous emission rate is maximum for  $D/\lambda \sim 0.245$  when the quantum dot efficiently couples to the fundamental waveguide mode and the emission is well confined in the nanowire. At smaller nanowire diameters, we observe an inhibition of the spontaneous emission by a factor of 12, from which we obtain a radiative quantum efficiency exceeding 92% for quantum dots in bottom-up grown nanowires.

This work was supported by the Netherlands Organization for Scientific Research (NWO), Dutch Organization for Fundamental Research on Matter (FOM), European Research Council and DARPA QUEST grant.

- <sup>1</sup>J. Claudon, J. Bleuse, N. S. Malik, M. Bazin, P. Jaffrennou, N. Gregersen, C. Sauvan, P. Lalanne, and J.-M. Gerard, *Nature Photon.* **4**, 174 (2010).  
<sup>2</sup>M. E. Reimer, G. Bulgarini, N. Akopian, M. Hocevar, M. Bouwes Bavincq, M. A. Verheijen, E. P. A. M. Bakkers, L. P. Kouwenhoven, and V. Zwiller, *Nat. Commun.* **3**, 737 (2012).

- <sup>3</sup>T. M. Babinec, B. J. M. Hausmann, M. Khan, Y. Zhang, J. R. Maze, P. R. Hemmer, and M. Loncar, *Nature Nanotechnol.* **5**, 195 (2010).  
<sup>4</sup>I. Friedler, C. Sauvan, J. P. Hugonin, P. Lalanne, J. Claudon, and J. M. Gerard, *Opt. Express* **17**, 2095 (2009).  
<sup>5</sup>J. Bleuse, J. Claudon, M. Creasey, N. S. Malik, J.-M. Gerard, I. Maksymov, J.-P. Hugonin, and P. Lalanne, *Phys. Rev. Lett.* **106**, 103601 (2011).  
<sup>6</sup>J. Heinrich, A. Huggenberger, T. Heindel, S. Reitzenstein, S. Höfling, L. Worschech, and A. Forchel, *Appl. Phys. Lett.* **96**, 211117 (2010).  
<sup>7</sup>D. Dalacu, K. Mnaymneh, X. Wu, J. Lapointe, G. C. Aers, P. J. Poole, and R. L. Williams, *Appl. Phys. Lett.* **98**, 251101 (2011).  
<sup>8</sup>A. Pierret, M. Hocevar, S. L. Diedenhofen, R. E. Algra, E. Vlieg, E. C. Timmering, M. A. Verschuuren, G. W. G. Immink, M. A. Verheijen, and E. P. A. M. Bakkers, *Nanotechnology* **21**, 065305 (2010).  
<sup>9</sup>M. H. M. van Weert, N. Akopian, U. Perinetti, M. P. van Kouwen, R. E. Algra, M. A. Verheijen, E. P. A. M. Bakkers, L. P. Kouwenhoven, and V. Zwiller, *Nano Lett.* **9**, 1989 (2009).  
<sup>10</sup>L. E. Jensen, M. T. Björk, S. Jeppesen, A. I. Persson, B. J. Ohlsson, and L. Samuelson, *Nano Lett.* **4**, 1961 (2004).  
<sup>11</sup>M. T. Borgstrom, G. Immink, B. Ketelaars, R. Algra, and E. P. A. M. Bakkers, *Nature Nanotechnol.* **2**, 541 (2007).  
<sup>12</sup>M. Gong, W. Zhang, G. C. Guo, and L. He, *Appl. Phys. Lett.* **99**, 231106 (2011).  
<sup>13</sup>M. Fujita, S. Takahashi, Y. Tanaka, T. Asano, and S. Noda, *Science* **308**, 1296 (2005).  
<sup>14</sup>W.-H. Chang, W.-Y. Chen, H.-S. Chang, T.-P. Hsieh, J.-I. Chyi, and T.-M. Hsu, *Phys. Rev. Lett.* **96**, 117401 (2006).  
<sup>15</sup>P. Lodahl, A. F. van Driel, I. S. Nikolaev, A. Irman, K. Overgaag, D. Vanmaekelbergh, and W. L. Vos, *Nature* **430**, 654 (2004).  
<sup>16</sup>M. D. Leistikow, A. P. Mosk, E. Yeganegi, S. R. Huisman, A. Lagendijk, and W. L. Vos, *Phys. Rev. Lett.* **107**, 193903 (2011).